Recent results from kaon physics

Giuseppe Ruggiero[*†]

Lancaster University

E-mail: giuseppe.ruggiero@cern.ch

The $\pi\nu\nu$ is one of the theoretically cleanest meson decay where to look for indirect effects of new physics complementary to LHC searches. The NA62 experiment at CERN SPS is designed to measure the branching ratio of the $K^+ \to \pi^+ \nu\bar{\nu}$ decay with 10% precision. NA62 took data in 2015 and 2016 reaching the Standard Model sensitivity. The KOTO experiment in Japan is investigating the decay $K_L \to \pi^0 \nu\bar{\nu}$ reaching a higher background suppression. Both experiments are reviewed, and recent results and prospects are summarised.

1. Introduction

The $K^+ \to \pi^+ \nu \bar{\nu}$ and $K_L \to \pi^0 \nu \bar{\nu}$ are flavour changing neutral current decays proceeding through box and electroweak penguin diagrams. A quadratic GIM mechanism and a strong Cabibbo suppression make these processes extremely rare. Using the value of tree-level elements of the Cabibbo-Kobayashi-Maskawa (CKM) triangle, the Standard Model (SM) predicts [1, 2]:

$$BR(K^+ \to \pi^+ \nu \bar{\nu}) = (8.4 \pm 1.0) \times 10^{-11} \quad BR(K_L \to \pi^0 \nu \bar{\nu}) = (3.4 \pm 0.6) \times 10^{-11}.$$

The knowledge of V_{cb}, V_{ub} and the CKM angle γ dominate the uncertainties. The theoretical accuracy, instead, is at percent level because: short distance physics dominates due to the top quark loop exchange; the hadronic matrix elements cancel in the normalization of the $\pi \nu \nu$ branching ratios (BR) to the measured $K^+ \to \pi^0 e^+ \nu$ BR. The dependence on the CKM elements partially cancels in the correlation between $K^+ \to \pi^+ \nu \bar{\nu}$ and $K_L \to \pi^0 \nu \bar{\nu}$. Therefore simultaneous measurements of the two BRs' would allow a theoretical clean exploitation of the CKM triangle using kaons only.

The $\pi \nu \nu$ decays are very sensitive to physics beyond the SM, probing the highest mass scales among the rare meson decays [3, 4, 5, 6, 7]. Despite the strong constraints on new physics from LHC, significant modifications of the SM values of the $\pi \nu \nu$ BRs' induced by new physics at mass scales up to 100 TeV are possible providing BRs' measurements with 10% precision at least.

The experimental status is [8, 9, 10]:

$$BR(K^+ \to \pi^+ \nu \bar{\nu})_{exp} = \left(17.3^{+11.5}_{-10.5}\right) \times 10^{-11} \quad BR(K_L \to \pi^0 \nu \bar{\nu})_{exp} < 2.6 \times 10^{-8} \ \ 90\% \ CL.$$

The charged mode has been observed by stopping kaon experiments. Still 3 order of magnitude need to be covered to observe the neutral mode.

2. NA62 experiment at CERN

The NA62 experiment at CERN [11, 12, 13] aims to measure the $K^+ \to \pi^+ \nu \bar{\nu}$ BR with 10% precision. Therefore it needs to collect about 10^{13} kaon decays using 400 GeV/c protons from SPS for a 10% signal acceptance. Keeping the background to signal ratio about 10% requires the use of almost independent experimental techniques to suppress unwanted final states. With a single event sensitivity of 10^{-12} NA62 can afford also a broader physics program [14]. NA62 is running with the apparatus fully operational since 2016.

NA62 adopts a kaon decay-in-flight technique. Fig. 1 shows a schematic view of the apparatus. Primary SPS protons strike a target from which a secondary charged hadron beam of 75 GeV/c and 1% momentum bite is selected and transported to the decay region. The detailed descriptions of the apparatus can be found in [13]. The incoming kaon is positively identified by a differential Cerenkov counter (KTAG) and its momentum and direction are measured by three stations of Si pixel detectors (GTK). About 6% of beam particles are K^+. A guard ring detector (CHANTI) vetoes beam inelastic interactions occurring in GTK. A decay tank, holding a 10^{-6} mbar vacuum, is surrounded by lead-glass annular calorimeters (LAV) designed to catch photons up to 50 mrad. Four stations of straw chambers (STRAW) in vacuum trace downstream charged particles, with a dipole magnet providing a 270 MeV/c transverse kick for momentum analysis. A RICH counter
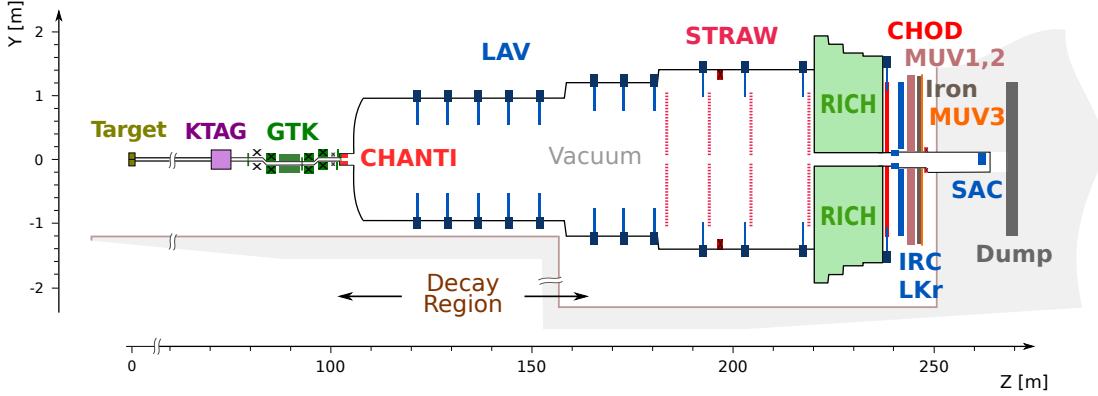
Figure 1: Schematic layout of the NA62 experiment in the *yz* plane.

time-stamps and identifies charged particles; plastic scintillators (CHOD) are used for triggering and timing. Photon rejection in the forward region is provided by: an electromagnetic calorimeter at liquid krypton (LKr); small angle calorimeters (IRC and SAC). Hadron calorimeters (MUV1,2) and a plastic scintillator detector (MUV3) are used to suppress muons. The SPS delivers 3.3×10^{12} protons per pulse at full intensity to NA62, corresponding to 750 MHz particle rate in GTK. Information from CHOD, RICH, MUV3 and LKr are built up online to issue level zero trigger conditions. Software-based variables from KTAG, CHOD, LAV and STRAW provide higher level trigger requirements. $K^+ \rightarrow \pi^+ \nu\bar{\nu}$-triggered data are taken concurrently with downscaled samples of data for rare kaon decays studies and minimum bias.

The NA62 apparatus has been commissioned in 2015 and 2016. Low intensity data have been taken in 2015 with a minimum bias trigger to study detector performances and to perform physics analysis. In fall 2016 NA62 has collected about 4.5×10^{11} kaon decays for $K^+ \rightarrow \pi^+ \nu\bar{\nu}$ at 20-40% of nominal intensity. A 4-months run dedicated to $K^+ \rightarrow \pi^+ \nu\bar{\nu}$ has taken place in 2017 at 50-60% of the nominal intensity and another one is scheduled in 2018.

2.1 Principle of the $K^+ \rightarrow \pi^+ \nu\bar{\nu}$ Measurement

The signature of the signal is one track in the initial and one in final state. The main kinematic variable is $m_{miss}^2 \equiv (P_K - P_{\pi^+})^2$, with P_K and P_{π^+} 4-momenta of K^+ and of the charged decay product under the π^+ mass hypothesis, respectively. Fig. 2 shows the m_{miss}^2 theoretical shape of the most important K^+ decay modes compared to $K^+ \rightarrow \pi^+ \nu\bar{\nu}$. Signal regions are defined between $K^+ \rightarrow \mu^+ \nu$ and $K^+ \rightarrow \pi^+ \pi^0$ and between $K^+ \rightarrow \pi^+ \pi^0$ and $K^+ \rightarrow \pi^+ \pi^+ \pi^-$. Non gaussian m_{miss}^2 resolution tails, radiative tails, $K^+ - \pi^+$ mis-matching and neutrinos in final states are the mechanisms inducing backgrounds from K^+ decays entering signal regions. Kinematics, timing, particle identification and photon rejection contribute to background suppression. The analysis is done with P_{π^+} between 15 and 35 GeV/c, so that π^0s' from $K^+ \rightarrow \pi^+ \pi^0$ can be hardly missed because of high energy.

2.2 $K^+ \rightarrow \pi^+ \nu\bar{\nu}$ Analysis

In this section a preliminary analysis of a 5% sub-sample of the 2016 data is described. The
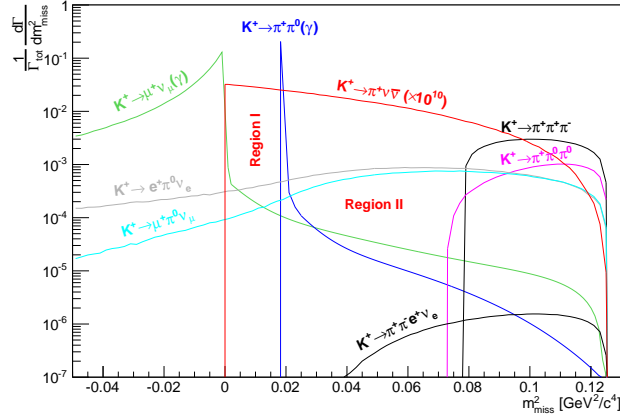
2

Figure 2: m_{miss}^2 shapes for signal and backgrounds of the main K^+ decay modes: the backgrounds are normalized according to their branching ratio; the signal is multiplied by a factor 10^{10}.

parent K^+ track is reconstructed and time-stamped in GTK with 100 ps resolution; the daughter π^+ track is reconstructed in STRAW. CHOD and RICH measure π^+ time with resolution below 100 ps. The pion is associated in time to a KTAG kaon signal. The timing and the closest distance of approach between GTK and STRAW tracks allow a precise $K^+ - \pi^+$ matching. The kaon mistagging probability at 40% of nominal intensity is below 2%, signal acceptance about 75%.

Decays are selected within a 50 m fiducial region beginning 10 m downstream to the last GTK station (GTK3) to reject events originated from interactions of beam particles in GTK and kaon decays upstream of GTK3. Fig. 3 (left) exemplifies the kinematics of the selected events. The resolution of m_{miss}^2 drives the choice of the boundaries of the signal regions. Reconstruction tails from $K^+ \to \pi^+\pi^0$, $K^+ \to \mu^+\nu$ and $K^+ \to \pi^+\pi^+\pi^-$ set the level of background in signal regions. To reduce it, signal regions are restricted to boxes within a 3D space, defined by the m_{miss}^2, the same quantity computed using the momentum of the particle measured by the RICH under π^+ hypothesis ($m(RICH)_{miss}^2$) and computed replacing the 3-momentum of the kaon measured by the GTK with the nominal 3-momentum of the beam ($m(No-GTK)_{miss}^2$). The probability for $K^+ \to \pi^+\pi^0$ ($K^+ \to \mu^+\nu$) to enter the signal regions is 6×10^{-4} (3×10^{-4}), as measured on data.

Calorimeters and RICH separate π^+, μ^+, e^+. A multivariate analysis combines calorimetric information and provides 10^5 μ^+ suppression and 80% π^+ efficiency. RICH quantities are used to infer particle types, giving 10^2 μ^+ suppression and 80% π^+ efficiency. The two methods are independent and therefore able to suppress μ^+ by 7 orders of magnitude while keeping 65% of π^+.

Left over events after π^+ identification are primarily $K^+ \to \pi^+\pi^0$. Photon rejection exploiting timing coincidences between π^+ and calorimetric deposits suppresses them further. The resulting π^0 rejection inefficiency is $(1.2 \pm 0.2) \times 10^{-7}$, as measured from minimum bias and $K^+ \to \pi^+\nu\bar{\nu}$-triggered events before and after γ rejection, respectively. Random losses are in the 15-20% range.

A sample of $K^+ \to \pi^+\pi^0$ from minimum bias is used for normalization. About 0.064 $K^+ \to \pi^+\nu\bar{\nu}$ events are expected over 2.3×10^{10} K^+ decays. Fig. 3 (right) shows the distribution of residual events in the $m(RICH)_{miss}^2$ versus m_{miss}^2 plane. Backgrounds from $K^+ \to \pi^+\pi^0$, $K^+ \to \mu^+\nu$ and $K^+ \to \pi^+\pi^+\pi^-$ are 0.024, 0.011 and 0.017, respectively. They are estimated directly from events outside signal regions, with the measured kinematic tails used for extrapolation in signal regions.
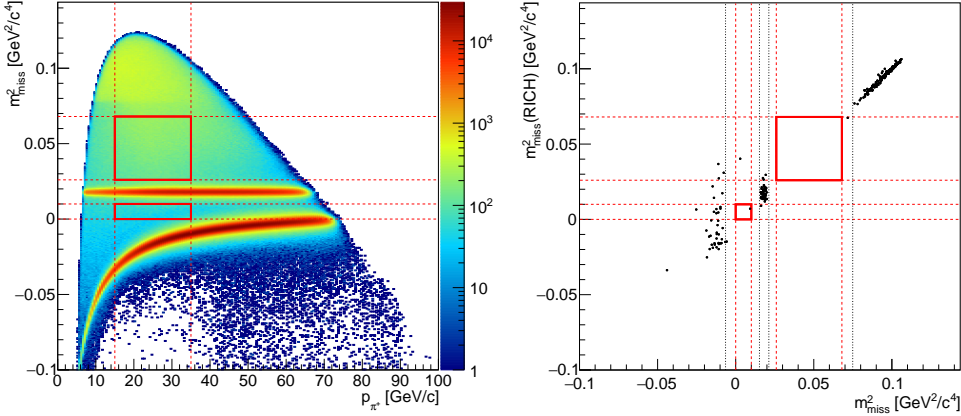
Figure 3: Distribution of m_{miss}^2 as a function of track momentum for events selected on minimum bias data; the bands corresponding to $K^+ \to \pi^+\pi^0$ and $K^+ \to \mu^+\nu$ decays are clearly visible; the signal regions (red box) are drawn for reference (left). Distribution in the $(m_{miss}^2(RICH), m_{miss}^2)$ plane of $K^+ \to \pi^+\nu\bar{\nu}$-triggered events passing the selection, except for the cut on $m_{miss}^2(No - GTK)$; signal regions (red tick boxes) and lines defining background regions (light dashed lines) are drawn; the event in region 1 has $m_{miss}^2(No - GTK)$ outside the signal region (right).

Simulations studies indicate that background from other processes is lower or negligible. The analysis is still on-going together with an optimization of the selection to further reduce backgrounds and increase signal acceptance. No events are observed in signal regions.

NA62 aims to reach the SM sensitivity from the analysis of the 2016 data and to select some tens of $K^+ \to \pi^+\nu\bar{\nu}$ events from the analysis of the data taken in 2017 and expected in 2018. Data taken after 2018 is being considered to complete the measurement.

3. KOTO experiment at J-PARC

KOTO [15] is a fixed target experiment at J-PARC [16] in Japan using protons from the Main Ring accelerator [17], aiming to observe few SM $K_L \to \pi^0\nu\bar{\nu}$ events.

A schematic view of the KOTO detectors is shown in fig. 4. Primary protons from the main ring (30 GeV/c) impinge on a target with 16 degree production angle. A secondary neutral hadron beam of 1.4 GeV/c peak momentum, composed by K^0, neutrons and photons is transported to a 3 m long decay region holding a vacuum of about 5×10^{-7} mbar. Photons detectors hermetically surround the decay volume. The entrance region of the decay volume is designed to minimize beam interactions in the collimators. Scintillator-lead sampling calorimeters at high angles provide photon rejection. A high-resolution electromagnetc calorimeter with crystals of CsI detects forward photons to reconstruct the kinematics of the signal π^0. The small angle region at the exit of the decay volume around the beam pipe is instrumented with plastic counters to veto mainly background from events with charged particles in final state. All the detectors are equipped with waveform digitizers readout to separate signals from pileup.

The first KOTO run took place in 2013 at an intensity of about 2×10^{13} proton per pulse, corresponding to 25 kW power delivered by JPARC. Then KOTO ran in 2015 and 2016 at an
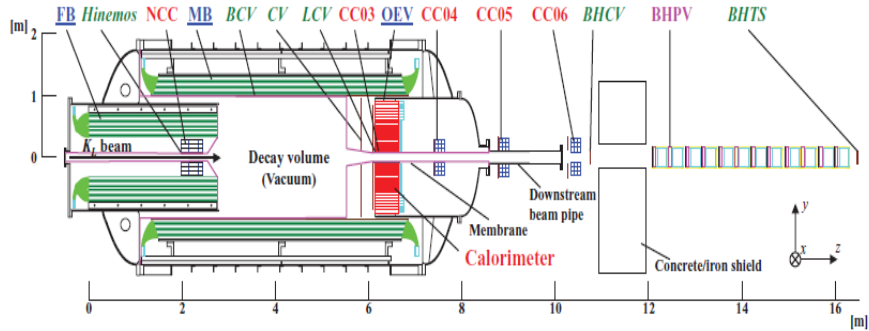
Figure 4: Schematic layout of the KOTO experiment in the *xz* plane.

intensity of 30-40 kW, collecting about 20 times the statistics of 2013.

3.1 Principle of the $K_L \rightarrow \pi^0 \nu \bar{\nu}$ Measurement

The signature of the signal is 2 γs' in the forward calorimeter. Under the π^0 mass hypothesis both the longitudinal coordinate of the decay vertex (Z_{vtx}) and the transverse momentum of the π^0 (p_T) can be determined, allowing the identification of a signal region (fig. 5). Rejection of backgrounds from $K_L \rightarrow \pi^0 \pi^0 (\pi^0)$ fully relies upon photon veto efficiency. Left over events mainly come from $K_L \rightarrow \pi^+ \pi^- \pi^0$ and neutron induced backgrounds originated from scattering and π^0 production at the entrance. Suppression of these backgrounds depends on the design of the entrance collimators, on the downstream plastic scintillators, on the shape of the calorimetric energy depositions of γ and neutron and on the distribution in the Z_{vtx} versus p_T plane.

3.2 2013 data analysis and result

KOTO has analyzed the full 2013 data set, corresponding to about 2.3×10^{11} K_L decays reaching a single event sensitivity (SES) of 1.3×10^{-8}. The number of expected events in signal region after the selection is 0.34 ± 0.16. One is observed, as shown in fig. 5 (right), leading to an upper limit on the $K_L \rightarrow \pi^0 \nu \bar{\nu}$ branching ratio $BR(K_L \rightarrow \pi^0 \nu \bar{\nu}) < 5.1 \times 10^{-8}$ at 90% C.L. [18]. The result is limited by backgrounds from neutron scattering, $K_L \rightarrow \pi^0 \pi^0$ and $K_L \rightarrow \pi^+ \pi^- \pi^0$ to a lesser extent. The background is estimated using simulation overlaid with accidental hits collected with data and validated with $K_L \rightarrow \pi^0 \pi^0 (\pi^0)$ samples. The decay $K_L \rightarrow \pi^0 \pi^0$ is used for normalization. Systematic uncertainties come mainly from the evaluation of the acceptances both for signal and normalization and are taken into account in the final result. Despite the limit is almost two times worse than the best one obtained by the E931 experiment, this analysis has set the level of the sensitivity of KOTO, showing paths for improvements.

3.3 KOTO after 2013

A re-design of the entrance region and a better instrumentation of the beam pipe followed the
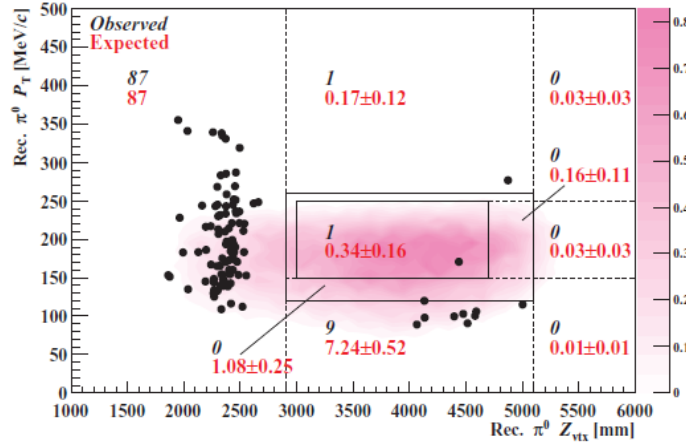
Figure 5: p_T versus Z_{vtx} of events with all the analysis cuts imposed. The region surrounded with a thick solid line is the signal region. The black dots represent the data and the contour indicates the distribution of the signal from Monte Carlo simulations. The black italic (red regular) numbers indicate the numbers of observed events (expected background events) for the regions divided by solid and dashed lines

2013 run. A special neutron-enriched run was taken to study the calorimeter response to neutrons, leading to a factor 5 improvement of the neutrons$-\gamma$s' separation in the CsI calorimeter [20].

A sub-sample of 2015 data comparable in size to the 2013 one is under analysis. The SES and the estimation background in signal region are 5.9×10^{-9} and 0.17 ± 0.05, respectively; a factor 2 lower than the 2013 analysis thanks to the hardware and software improvements. The 2015 analysis is currently under finalization.

The full 2015 and 2016 data samples correspond to 10^{-9} SES, allowing the Grossman - Nir limit [19] for a SM $K_L \to \pi^0 \nu \bar{\nu}$ decay to be reached. However both the data taken so far and the level of background are still not adequate to observe $K_L \to \pi^0 \nu \bar{\nu}$ events. To reach this goal several improvements on the detector side are on progress: a more efficient barrel photon veto installed and used in 2016 [20], modification of the beam pipe to reduce $K_L \to \pi^+ \pi^- \pi^0$ background, a dual both-end readout of the CsI calorimeter to better separate neutrons and γs', an increase of the J-PARC power up to 100 kW.

4. Conclusions

The kaon experiments NA62 at CERN and KOTO at J-PARC are running to search for physics beyond the SM through the ultra-rare $\pi \nu \nu$ decays. NA62 performances are within expectations. The experiment aims to reach the SM sensitivity for $K^+ \to \pi^+ \nu \bar{\nu}$ with the analysis of the data collected in 2016 and to get some tens of SM events exploiting data from 2017 and from the already scheduled 2018 run. Data taken after 2018 is being considered to complete the measurement. KOTO experiment is expected to cross the 10^{-9} single event sensitivity for $K_L \to \pi^0 \nu \bar{\nu}$ with the data taken in 2015 and 2016. Hardware refurbishments are ongoing aiming to the observation of few SM $K_L \to \pi^0 \nu \bar{\nu}$ events by 2021.

References

[1] J. Brod, M. Gorbahn and E. Stamou, *Phys. Rev. D* **83** (2011) 034030 [arXiv:1009.0947 [hep-ph]].

[2] A.J. Buras, D. Buttazzo, J. Girrbach-Noe and R. Knegjens, *JHEP* **1511** (2015) 33 [arXiv:1503.02693 [hep-ph]].

[3] M. Blanke, A.J. Buras and S. Recksiegel, *Eur. Phys. J. C* **76 no.4** (2016) 182 [arXiv:1507.06316 [hep-ph]].

[4] M. Blanke, A.J. Buras, B. Duling, K. Gemmler and S. Gori, *JHEP* **903** (2009) 108 [arXiv:0912.3803 [hep-ph]].

[5] A.J. Buras, D. Buttazzo and R. Knegjens, *JHEP* **1511** (2015) 166 [arXiv:1507.08672 [hep-ph]].

[6] G. Isidori, F. Mescia, P. Paradisi, C. Smith and S. Trine, *JHEP* **0608** (2006) 64 [hep-ph/0604074].

[7] M. Tanimoto and K. Yamamoto, *PTEP* **2015 no.5** (2015) 053B07 [arXiv:1503.06270 [hep-ph]].

[8] A.V. Artamonov *et al.* [E949 Collaboration], *Phys. Rev. Lett.* **101** (2008) 191802 [arXiv:0808.2459 [hep-ph]].

[9] A.V. Artamonov *et al.* [E949 Collaboration], *Phys. Rev. D* **79** (2009) 092004 [arXiv:0903.0030 [hep-ph]].

[10] J.K. Ahn *et al.* [E391a Collaboration], *Phys. Rev. D* **81** (2010) 072004 [arXiv:0911.4789 [hep-ph]].

[11] A. Anelli *et al.*, CERN-SPSC-2005-013; SPSC-P-326.

[12] NA62 Technical Design Document NA62-10-07; https://cdsweb.cern.ch/record/14049857.

[13] E. Cortina Gil *et al.* [NA62 Collaboration], *JINST* **12** no. 05 (2017) P05025 [arXiv:1703.08501 [hep-ph]].

[14] G. Ruggiero, in proceedings of KAON 2016 conference, J. Phys. Conf. Ser. **800** (2017) no.1 012023.

[15] T. Yamanaka [KOTO Collaboration], *PTEP* **2012** (2012) 02B006.

[16] S. Nagamiya, *PTEP* **2012** (2012) 02B001.

[17] T. Koseki *et al.*, *PTEP* **2012** (2012) 02B004.

[18] J.K Ahn *et al.* [KOTO Collaboration], *PTEP* **2017 no.2** (2017) 021C01 [arXiv:1609.03637 [hep-ph]].

[19] Y. Grossman and Y. Nir, *Phys. Lett. B* **398** (1997) 163 [hep-ph/9701313].

[20] K. Shiomi, in proceedings of KAON 2016 conference, J. Phys. Conf. Ser. **800** (2017) no.1 012022.